CEBAF PROPOSAL COVER SHEET

This Proposal must be mailed to:

CEBAF
Scientific Director's Office
12000 Jefferson Avenue
Newport News, VA 23606

and received on or before OCTOBER 30, 1989

TITLE:

Deuteron Photodisintegration

CONTACT PERSON:

David A. Jenkins

ADDRESS, PHONE AND BITNET:

Physics Department   703-231-6712
Virginia Tech   Jenkins@VTVM2
Blacksburg, VA 24061

THIS PROPOSAL IS BASED ON A PREVIOUSLY SUBMITTED LETTER OF INTENT

☒ YES
☐ NO

IF YES, TITLE OF PREVIOUSLY SUBMITTED LETTER OF INTENT

Deuteron Photodisintegration

ATTACH A SEPARATE PAGE LISTING ALL COLLABORATION MEMBERS AND THEIR INSTITUTIONS

===
(CEBAF USE ONLY)

etter Received___10-31-89_____

og Number Assigned___PR-89-020_____

y_____KES_____

Deuteron Photodisintegration

D. A. Jenkins
Virginia Tech

S. T. Thornton, R. Sealock, O. Rondon-Aramayo, S. Hoblit
University of Virginia

K. Giovanetti
James Madison University

V. Burkert, B. Mecking and R. Whitney
CEBAF

Wade Sapp
Massachusetts Institute of Technology

Photon Tagging Group
Arizona State University
Carnegie Mellon University
Catholic University
George Washington University
University of South Carolina

Abstract

We propose to measure the differential cross section and polarization parameters for photodisintegration of the deuteron at CEBAF over a wide range of angles for energies up to 2.5 GeV. The experiment combines a well known probe, the photon, with exact nuclear wave functions to test models of the nucleus. The experiments will provide basic data for testing detailed theories of nucleon structure and the nucleon interaction without involving the complexities associated with heavier nuclei. By examining the reaction for the range of energies and angles available with a tagged beam at CEBAF, the experiment will explore new phenomena for nuclear physics.

Photodisintegration

The photodisintegration of the deuteron is one of the most fundamental processes which can be investigated in nuclear physics. The deuteron, being the simplest of all nuclear systems, has the same importance for nuclear theory that the hydrogen atom has for atomic theory. At energies below 1 GeV, experimental and theoretical studies of this reaction have given important information about the wave function of the deuteron at small internucleon distances. The reaction is sensitive to contributions of various mechanisms such as meson exchange, the excitation of isobars and relativistic effects. At energies above 1 GeV there is an expectation that the reaction will enter a regime where quark effects will become important.

We propose a program of experiments to measure the differential cross section and polarization observables for the photodisintegration of the deuteron. The proposed tagged beam at CEBAF will allow the study of this reaction at energies and with polarizations which have not been available thus far. The goal of the experimental program is to measure as many parameters of the reaction as possible in order to constrain the amplitudes which describe the process and thus provide a definitive test of nuclear models. The experiments will test theoretical models of the deuteron from low energies where pion exchange phenomena are dominant to high energies where quark phenomena are expected to appear.

Real photons complement electron scattering experiments which explore the nucleus with virtual photons. However there are a number of experiments for which the real photon probes the nucleus in a domain which is not easily accessible by electrons. For example, deuteron photodisintegration leads to two particle final states which simplifies the reconstruction of kinematics for the reaction. Whereas photodisintegration is described by twelve helicity amplitudes, electrodisintegration requires eighteen amplitudes and is more complicated for theoretical analysis. In addition photodisintegration experiments can use frozen spin targets that would be damaged in electrodisintegration experiments. Frozen spin targets have the advantage of containing fewer impurities thereby reducing unwanted reactions in the target.

The photon has not been widely used as a nuclear probe because of the difficulties presented by low-intensity and poor-duty-cycle beams and by the low cross sections for interaction in the presence of large backgrounds. Much of the present photodisintegration data has been taken with bremsstrahlung beams with which the determination of absolute cross sections is difficult because of errors associated with the measurement of the flux and bremsstrahlung spectral profile.

CEBAF is unique in that the photon tagger and large acceptance of the CLAS detector will allow measurements at small cross section over a broad energy range. In addition spin measurements can be performed with both linearly polarized and circularly polarized photons, polarized targets and a polarimeter for observing recoil nucleon polarization. There is no other accelerator in the world, present or planned, which can duplicate these facilities.

Experimental Measurements

A large body of data has accumulated for photodisintegration experiments up to 1 GeV. Results have been reported with both bremsstrahlung beams and tagged photons.

Many measurements have been made for the reaction in the Δ resonance region. Differential cross sections have been measured at Bonn[1], Tokyo[2], Bates[3] and Frascati[4]. Measurements of asymmetries using polarized photons exist in this region for angles from 70° to 150°. Recoil proton polarizations have been measured for three angles with energies from 200 MeV to 450 MeV at Stanford[5], and for two angles in the energy range from 282 MeV to 405 MeV at Bonn[6].

At energies above the Δ resonance region, extensive measurements up to 600 MeV have been made at Tokyo of the differential cross section[2], recoil polarization[7] and asymmetries using a vector polarized deuterium target[8]. Ching and Schaerf measured the photodisintegration of the deuteron from 500 to 1000 MeV at center-of-mass angles from 70° to 130°.[9]. Measurements have been reported at the California Institute of Technology[10] from 500 to 900 MeV and at Lund[11] from 139 to 832 MeV. A polarized target was used at Bonn to measure the target asymmetry at a photon energies of 450, 550 and 650 MeV and proton center-of-mass angles from 25° to 155°.[12] Measurements with polarized photons[13] were extended to higher energies at Kharkov[14,15] and Erevan[16]. The large value for the proton polarization was confirmed[17] and led to speculation about the existence of a dibaryon state.[7] Measurements of the differential cross section at 90° have been performed at SLAC in the energy range between 0.8 and 1.6 GeV; the SLAC data is presented in Fig. 1.[18] Future measurements in this energy range are planned at Bonn for energies up to 1 GeV with polarized targets and polarized photons.[19]

The reverse reaction has been studied by radiative capture measurements with polarized neutron fluxes in the energy range $100 < E_n < 600$ MeV at the Indiana University Cyclotron Facility[20] and
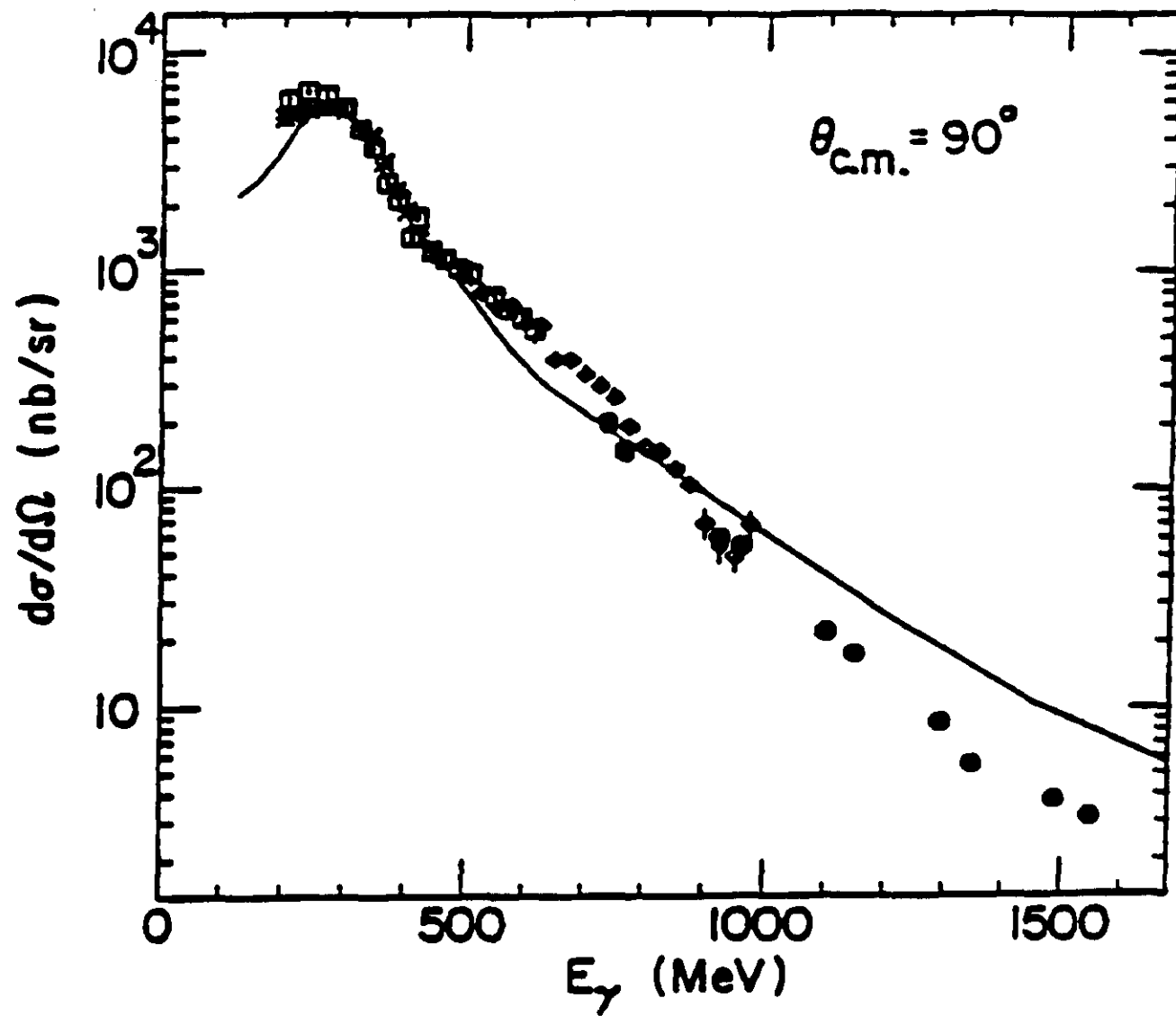
Figure 1. SLAC data: Comparison of SLAC data (solid points) with earlier data and with meson exchange calculation (solid line).

at TRIUMF[21]. In a review of this data, De Sanctis concludes that there is good agreement with the photodisintegration data.[22]

The experimental situation has been summarized by Cameron:[23]

"Major disparities between various measurements of the same observable are often present; however, in many cases the more recent measurements of cross sections yield absolute values that are consistent to better than 20%..... The recent measurement of many observables in deuteron photodisintegration at $E_\gamma > 400$ MeV has shown that models incorporating two dibaryon resonances, first introduced to explain the proton polarization, fail to reproduce the more extensive data set. Attempts to understand the underlying hard-scattering continuum have been initiated, and make apparent the need for data at higher energies."

The past history of these measurements indicates that great care is required to determine the cross section to better than 5%. We propose to begin a program that will extend the data set to higher energies and a wider angular range with instrumentation that will minimize systematic errors. The program would eventually include the use of polarized beams, polarized targets and polarimeters for measuring the polarization of the recoil proton and neutron.

Theory

The subject of deuteron photodisintegration has received considerable attention from theorists. Pfeil has calculated the differential cross section at high energies using an isobar model and Feynman graph techniques,[24] while Leidemann and Arenhovel have calculated the cross sections up to 1 GeV with a coupled channel approach.[25] These and other calculations achieve some agreement with experiment but more work will be needed before the reaction is understood. Inclusion of NNπ final state interactions is expected to give better agreement. There are two energy regions of special interest—around 700 MeV where resonances have been found in polarization data and above 1 GeV where QCD effects may be seen.

Resonance Phenomena

Several experiments have reported resonance effects in experiments between 500 and 800 MeV. Ogawa et al calculated the proton polarization for two models, a covariant model and a phenomenological model, in this energy range.[26] Diagrams for the reaction are shown in Fig. 2; the Born terms are given in Fig. 2a and 2b and the isobar resonance term for the Δ(1236) and
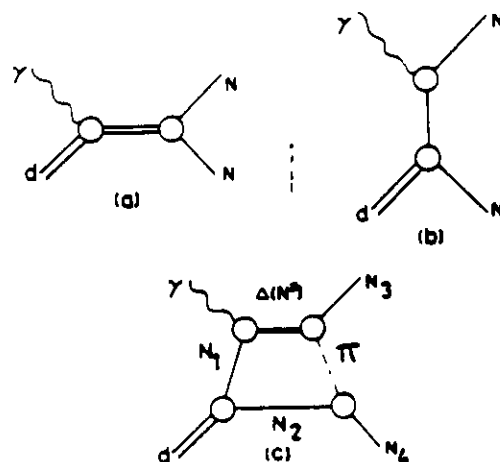
3

Figure 2. Feynman diagrams for the covariant analysis of deuteron photodisintegration. (a) deuteron-pole term, (b) nucleon-pole term, (c) resonance term.
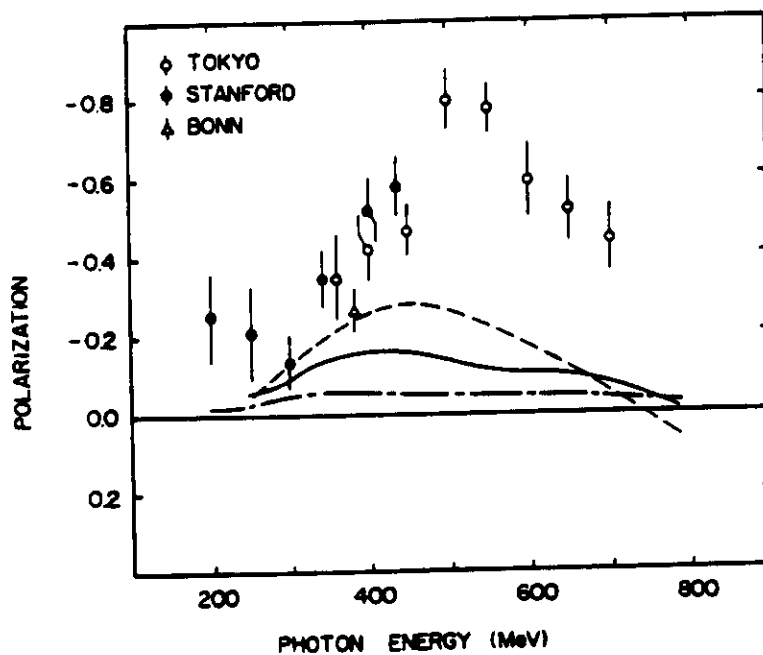

Figure 3. Proton polarization for the center-of-mass angle around 90°. Curves are the results of the theoretical calculations. The dot-dashed curve is from a covariant analysis whereas the solid curve and dashed curves are from a phenomenological analysis.

N*(1470) are given in Fig. 2c. The covariant model is an extension of conventional diagrammatic techniques for the computation of Born terms and isobar excitations. This model has large ambiguities since the γNN* coupling strengths for higher nucleon and delta resonances are not well known. The phenomenological model uses helicity amplitudes for real γN → N* → Nπ processes and is more easily extended to higher energies.

The results of calculations are shown in Fig. 3 which compares the theoretical models with polarization measurements. They find that, although their models give satisfactory agreement with the differential cross section data, none of the models give a satisfactory fit to the polarization data. In order to fit the polarization data, they suggest that the models should include a resonance term such as a dibaryon.

The existence of a dibaryon resonance is controversial. The first suggestion of their presence in experiment came from an analysis of the Λp invariant mass distribution by Dahl[27] and the discovery of a $^1D_2$ state* in an NN partial-wave analyses by Arndt[28]. At one time the dibaryon was thought to be a 6-quark state, but it is now regarded as a resonance in an NΔ or πNN intermediate state. A recent result of Shypit et al claims to have conclusively ruled out any broad dibaryon resonances in the NN $^1D_2$, $^3F_3$ and $^3P_2$ waves with masses between about 2100 and 2250 MeV.[29] However Hidaka, after reviewing the work of Shypit, states that their conclusion was based on an unfounded assumption that the branching ratio of the dibaryon to NΔ is large.[30] Whatever the outcome of the dibaryon controversy, the problem here is to understand the resonance-like behavior in the NN system observed in photodisintegration.

QCD Predictions
There are three predictions by QCD for photodisintegration cross sections. These predictions describe the magnitude of the helicity amplitudes, the momentum dependence of the differential cross section and the magnitude of a reduced nuclear amplitude.

Helicity amplitudes
QCD predicts that at high energies where perturbation theory is valid, the helicity of the nucleons should be conserved. Amplitudes which do not conserve helicity should be suppressed by a power of μ^2/p_T^2 where μ is a hadronic scale parameter and p_T is the transverse momentum.[31]

---

* Dibaryon states are represented by the notation $^{(2S+1)}L_J$ where S is the total spin, L is the orbital angular momentum and J the total angular momentum.

Since only three of the twelve helicity amplitudes describing the process conserve helicity, this prediction could be studied in spin experiments which study the energy dependence of the helicity amplitudes.

Constituent Counting Rules

The differential cross section for an exclusive process at fixed center-of-mass angle, by the rules of constituent counting, should approach the form $d\sigma/dt = 1/s^{n-2}$ where n is the total number of elementary fields.[32] For the present case with four nucleons and a photon, n = 13, so the quantity s^{11} $d\sigma/dt$ should approach a constant as the energy increases.

Reduced nuclear amplitude

Photodisintegration of the deuteron has been evaluated by Brodsky and Hiller using a model to account for nucleon structure in nuclear scattering amplitudes, consistent with quantum chromodynamics and covariance.[31] The differential cross section is written as

$$\frac{d\sigma}{d\Omega_{cm}} = \frac{1}{s - m_d^2} F_p^2(\hat{t}_p) F_n^2(\hat{t}_n) \frac{1}{p_T^2} f^2(\theta_{cm})$$

where

$$\hat{t}_i = (p_i - \tfrac{1}{2} p_d)^2$$

and the nucleon elastic form factor is approximated by the dipole formula

$$F_N(\hat{t}) = \frac{1}{\left(1 - \frac{\hat{t}}{0.71 Gev^2}\right)^2}$$

The remaining function $f^2(\theta_{cm})$ is defined by Brodsky and Hiller as the reduced nuclear scattering amplitude. This amplitude tends to remove the fall-off of the cross section due to the internal degrees of freedom of the nucleons. Using this model and normalizing the cross section to the data of Ching and Schaerf,[9] one obtains the cross sections plotted in Figure 4. Although the Brodsky-Hiller model may not be justified at these energies, it is the only theory available for estimating cross sections above the 1.5 GeV SLAC measurements.

Summary

The SLAC data is consistent with quark counting rules which predict an s^{-11} dependence for the

$\gamma\, d \to n\, p$ Cross Section

$\Theta_{cm} = 90°$

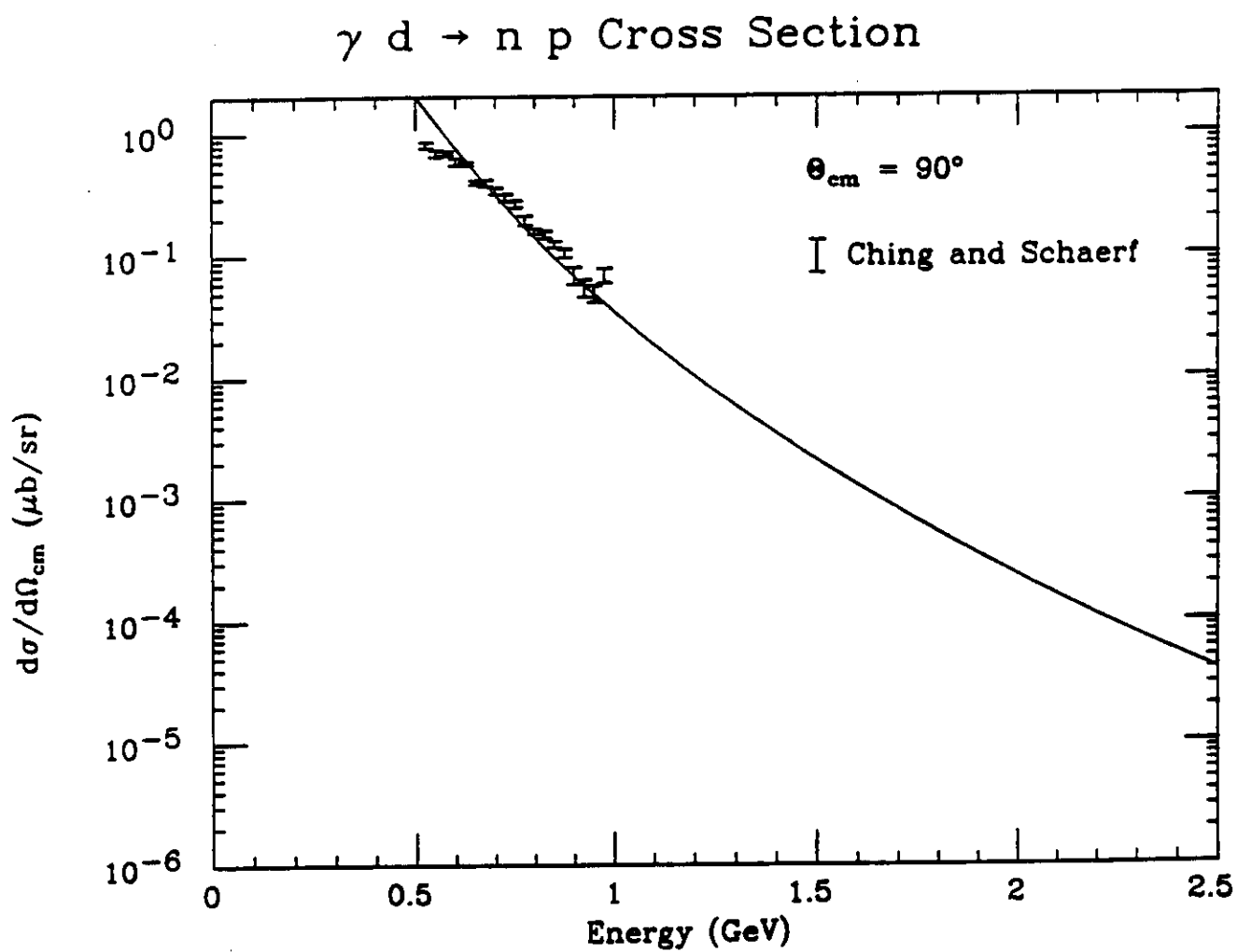$\mathbf{I}$ Ching and Schaerf

Figure 4. Differential cross section for deuteron photodisintegration

cross section. The comparison with the data, presented in Fig. 5, suggests the onset of quark effects in the nucleus for energies above 1 GeV. The Brodsky-Hiller model is in somewhat poor agreement with the results at higher energy, but this model is not ruled out by these data. Isgur and Smith warn that some care should be used when applying perturbative QCD in this energy domain.[33] In a consideration of deuteron electrodisintegration, Carlson and Gross find that, whereas the results of QCD and classical nuclear physics can be similar for differential cross sections, the predictions for individual helicity amplitudes can be dramatically different.[34] The study of helicity amplitudes by spin measurements should be equally important in seeing QCD effects in photodisintegration.

A Program of Study

We propose to begin a program of experiments with the CLAS detector to measure a set of observables which will place constraints on the 12 helicity amplitudes for the process. Experiments at a common energy with polarized beams, polarized targets and polarization measurements of the recoil neutron and proton would constrain these amplitudes and be an important part of a program of experiments that would provide a full range of observables for the comparison of experiment and theory.

I. Polarized Photons

The photon beam planned for CEBAF will be produced by placing a radiator in the electron beam to produce a photon beam in the forward direction.[35] The energy of electrons which produce photons in the radiator is measured by a magnetic spectrometer. The photon energy is then the difference in energy between the electron beam energy and the energy of the electron measured by the magnetic spectrometer. Each of the photons in the beam is thereby tagged by its energy.

In the standard configuration, the acceptance aperture of the tagging spectrometer and the photon reaction target are located symmetrically about the axis defined by the incident electron beam. The photon beam then contains all polarizations equally , and is, therefore, unpolarized. There are three ways to produce polarized photons—off-axis production, coherent production and production with polarized electrons. The first two methods produce linearly polarized photons while the last produces photons which are circularly polarized.

   A. Linear polarization—off-axis photons
      Photons produced by a beam of unpolarized electrons exhibit a partial linear polarization when observed at an angle away from the production axis. This polarization can
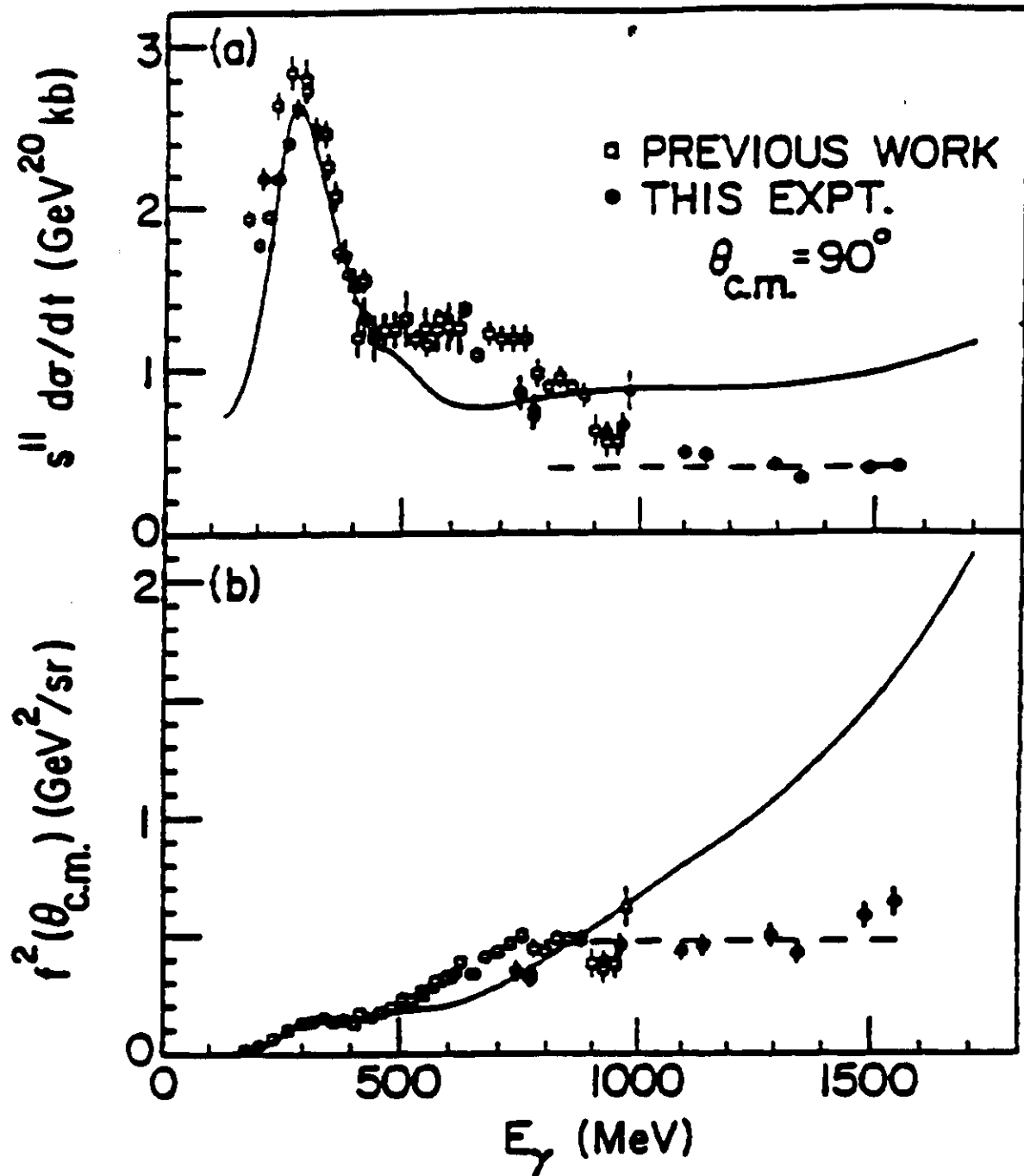
Figure 5. Comparison of SLAC data to quark model prediction : a) Cross section data illustrating s^{-11} dependence for data above 1 GeV. The solid curve represents a meson-exchange calculation while the dashed line represents an s^{-11} dependence. b) Reduced nuclear amplitude in the Brodsky-Hiller model. The solid curve is a meson-exchange calculation while the dashed line represents a constant energy dependence as expected in the Brodsky-Hiller model.

be greatly enhanced, as suggested by Laszewcki[36], by making a kinematic selection of the residual electrons used for tagging.

The use of this method at CEBAF would produce polarizations of the order of 50%. However the method requires accurate definition of the directions of the electron beam, the photon and the residual electron.

B. Linear polarization--coherent production

Polarized photons are also produced when an aligned crystal is used as a radiator. The polarized photons have an energy which is only a fraction of the electron beam energy, but high polarizations can be obtained. A disadvantage is that the polarization and intensity are not smooth functions of photon energy but rather a series of peaks with relative widths and intensities that are sensitive functions of the crystal parameters. Because the principal peak has a low energy, the tagging spectrometer must analyze energies approaching the beam energy.

C. Circular polarization

Since the CEBAF electron beam can be polarized, circularly polarized photon beams can be produced. These beams produce highly polarized photons over the CEBAF energy range.

II. Polarized Targets

Both vector and tensor polarized deuteron targets will be required for a complete set of polarization measurements. Since heating by energy loss in the target is quite low for tagged photon beams, frozen spin targets should be used to minimize reactions in the target material. The use of frozen spin targets and other polarization techniques for deuteron targets with tagged beams has been discussed by Meyer.[37]

III. Recoil Measurements

The polarization of the recoil particles can be measured by scattering in a carbon analyzer. This could be accomplished by inserting graphite slabs in the CLAS detector between the region 2 and region 3 drift chambers in order to track particles entering and leaving the slabs. The design of a polarimeter for analyzing recoil protons has been discussed by McNaughton[38] and the design of a polarimeter for recoil neutrons has been described by Madey et al.[39]

The neutron polarization could be measured by first recording the track of the proton from photodisintegration. Since the reaction is a two body process, the direction of the neutron and its position in a graphite polarimeter could be determined from the proton direction. The drift chambers behind the polarimeter could then be searched for a recoil proton from the neutron interaction in the graphite. The direction of the recoil proton would be correlated with the polarization of the neutron.

The first phase of the proposed program will measure differential cross sections and cross-section asymmetry with a linearly polarized beam.

Differential Cross Section

The differential cross section can be measured by identifying the proton from the reaction since this is a two body interaction and the beam energy will be known to 3 MeV by the tagging counters. The CLAS will have an angular acceptance which will extend from 8° to 150°. If necessary the associated neutron can be counted in the scintillation counters with an efficiency of 5% and in shower counters which will cover forward angles to 45° and to 90° in one sector. The shower counters will have an efficiency for neutrons of 50%.

A trigger for an event will be a proton count in one of the scintillators. After a trigger has been received, the wire chambers can be examined to record the trajectory of the track of the proton and verify that the trigger is associated with a two-body final state. The neutron counters could be used for a more positive event identification if accidental rates are high such as when measuring the reaction at high energies, at backward angles or when using polarized targets. A trigger for an event would then be a count in a tagging counter and counts in the neutron and proton counters.

The kinetic energy of the proton and neutron for different photon energies is plotted in Fig. 6. For the angular range of the CLAS, the experiment must detect protons with energies from 0.1 GeV to 2.2 GeV. The higher energy protons are produced only at extreme forward angles; the kinetic energy of the proton for high energy photons falls off rapidly with increasing angle to an energy less than 1 GeV at 60°.

We propose to use 1.6 GeV electrons in the tagger with the tagging interval extending from 30% to 95% of the full beam energy. Thus the photon energy will vary from 0.5 GeV to 1.5 GeV. The count rate can be estimated as follows:

Tagged Beam Intensity = 5×10^6/sec for full tagged beam

$= 5 \times 10^5$/sec for 100 MeV energy bin

Target Thickness = 10 cm of liquid deuterium (1.6 gm/cm^2)

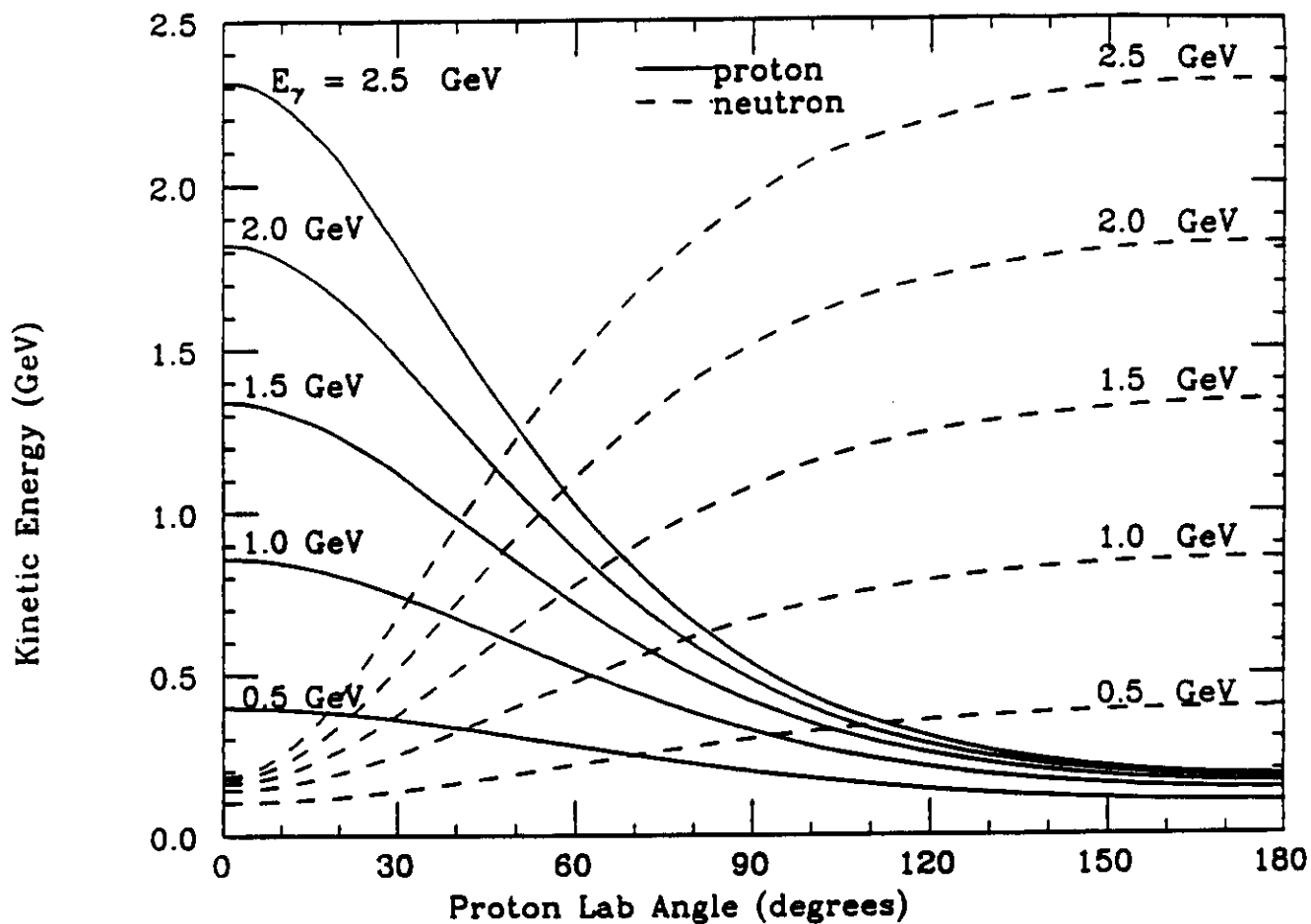Solid Angle = 9 sr

γ d → n p Kinematics

Figure 4. Reaction kinematics for deuteron photodisintegration: The solid line gives the proton kinetic energy as a function of proton angle for different incident photon energies. The dashed line gives the neutron kinetic energy as a function of proton angle for different incident photon energies.

Table I. Predicted rates in 100 MeV wide photon energy bins with no neutron counter coincidence requirement.

Energy GeV	$d\sigma/d\Omega$ nb/sr	Rate cts/hr	Rate in 20° bin cts/hr
0.55	700	5440	780
0.65	450	3500	500
0.75	200	1555	220
0.85	130	1010	144
0.95	80	622	89
1.05	30	233	33
1.15	20	155	22
1.25	10	78	11
1.35	6	47	7
1.45	4	31	4

If the cross section is 2 nb/sr, then

$$\text{Rate} = (5 \times 10^5/\text{sec})(2 \text{ nb/sr})(9 \text{ sr})(0.48 \text{ at/barn})$$

$$= 16 \text{ events/(hour-100 MeV energy bin)} \quad \text{(no neutron counter)}$$

Although the tagging system can operate at a rate a factor of ten higher, the beam intensity is limited by the high rate from three body processes discussed below. Rates predicted by the Brodsky differential cross section (Fig. 4) are given in Table I. The count rate calculation assumes that the differential cross section has no angular dependence and the incident photon flux is the same for all energies. Since the cross section decreases with increasing energy, the maximum energy achievable in the experiment will depend on background rates.

Other competing reactions

The maximum energy of particles created in other final states with a 2.5 GeV photon are shown in Fig. 7. The π^+nn reaction can produce high energy pions but these pions will be rejected by combining a momentum measurement in the spectrometer with a time-of-flight measurement.

There are several inelastic channels with large cross sections which will produce a high rate of protons in the counter system:

$$\gamma + d \rightarrow n + p + \pi^o$$

10
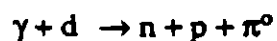
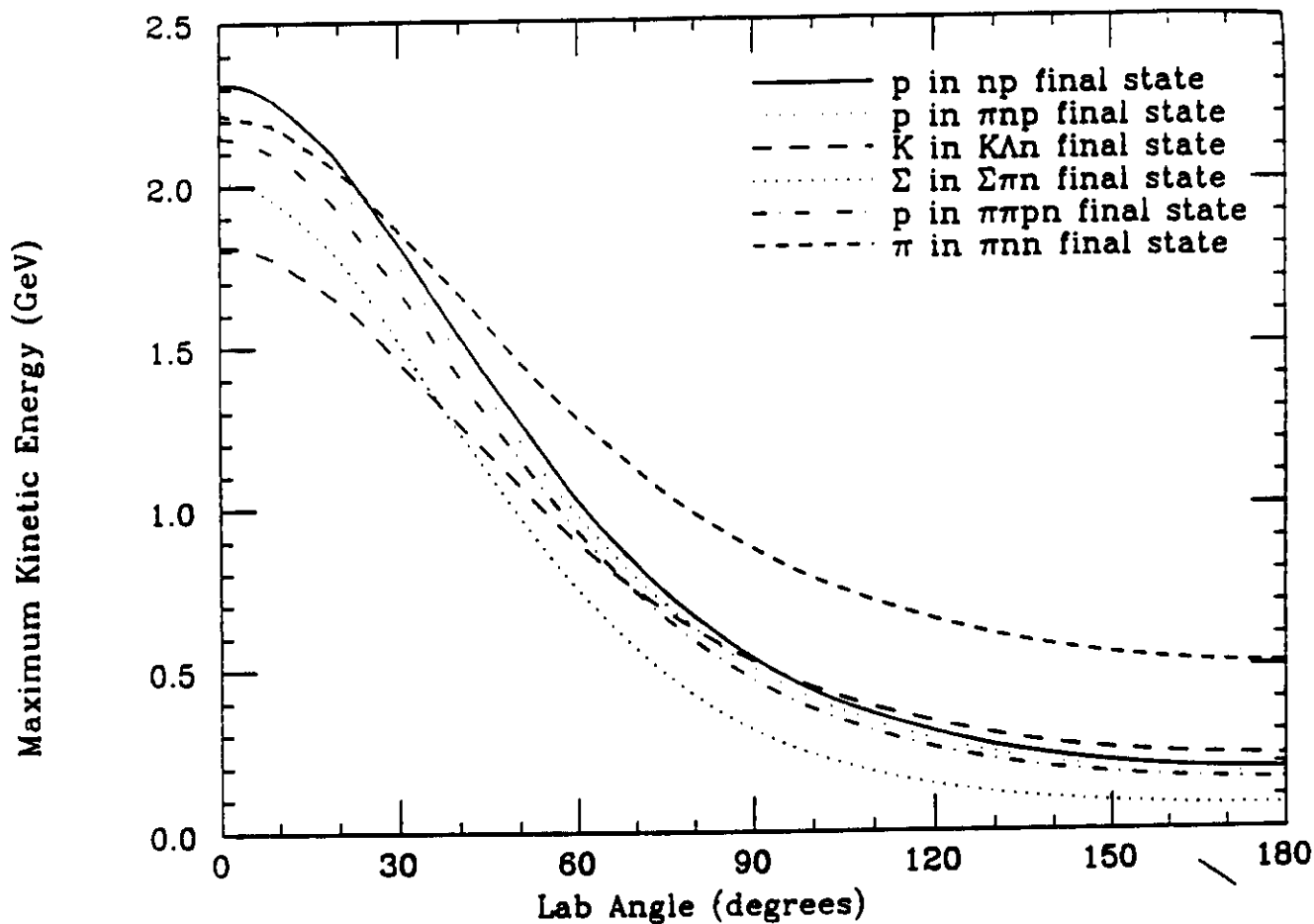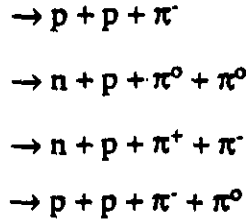# γd Reaction Kinematics, E_γ = 2.5 GeV

Figure 7. Energies for various final states of deuteron photodisintegration: The maximum energy for particles created in deuteron photodisintegration with 2.5 GeV photons is plotted as a function of lab angle.

$$\rightarrow p + p + \pi^-$$

$$\rightarrow n + p + \pi^o + \pi^o$$

$$\rightarrow n + p + \pi^+ + \pi^-$$

$$\rightarrow p + p + \pi^- + \pi^o$$

Each of these reactions can be separated from the direct channel by the fact that they produce a proton which has less energy than the proton in the two-body final state. For example, the energy difference of a proton in the direct channel and the $np\pi^o$ channel is plotted in Fig. 8. The energy difference for a 1.5 GeV photon varies between 70 MeV at 20° and 30 Mev at 150°. The proton energy at 150° for a 1.5 GeV photon is about 300 MeV. Thus with an energy resolution of 2% in the magnetic analysis of momentum, the proton energy will be measured to an accuracy of 6 MeV and can be easily resolved from the inelastic channel.

Trigger rates due to inelastic channels

The inelastic channel will be a more serious problem for those events produced by untagged photons with energies above the tagged photon energy. For example, if the primary electron beam energy is 1.6 GeV and the highest tagged photon has an energy of 1.5 GeV, the photons between 1.5 GeV and 1.6 Gev will produce high-energy protons in the inelastic channel which will contribute to the spectrum by accidental coincidences. The singles rate associated with this reaction can be estimated as follows:

Untagged photon intensity = 4×10^6/sec

Differential cross section= 1 μb/sr

Target density = 4.8×10^{23} at/cm^2

Singles rate=$(4\times10^6$/sec$)(10^{-30}$ cm^2/sr$)(9$ sr$)(4.8\times10^{23}$ at/cm$^2)$

=17/sec

The associated accidental rate can be calculated assuming a 2 ns resolving time between the scintillator trigger counters and the focal plane counters of the the tagger:

Accidental rate =$(17$/sec$)(5\times10^6$/sec$)(2\times10^{-9}$ sec$)$

= 612/hour

Since the reaction is a three body reaction, these protons will be spread out in energy and and appear as a continuum beneath the peak for the two-body process. However the rate is high and should be reduced if possible. Two steps would help: 1) a veto counter at the end of the focal plane to count electrons produced by photons at the upper end of the bremsstrahlung spectrum and 2) the inclusion in the event trigger of a counter immediately surrounding the target.
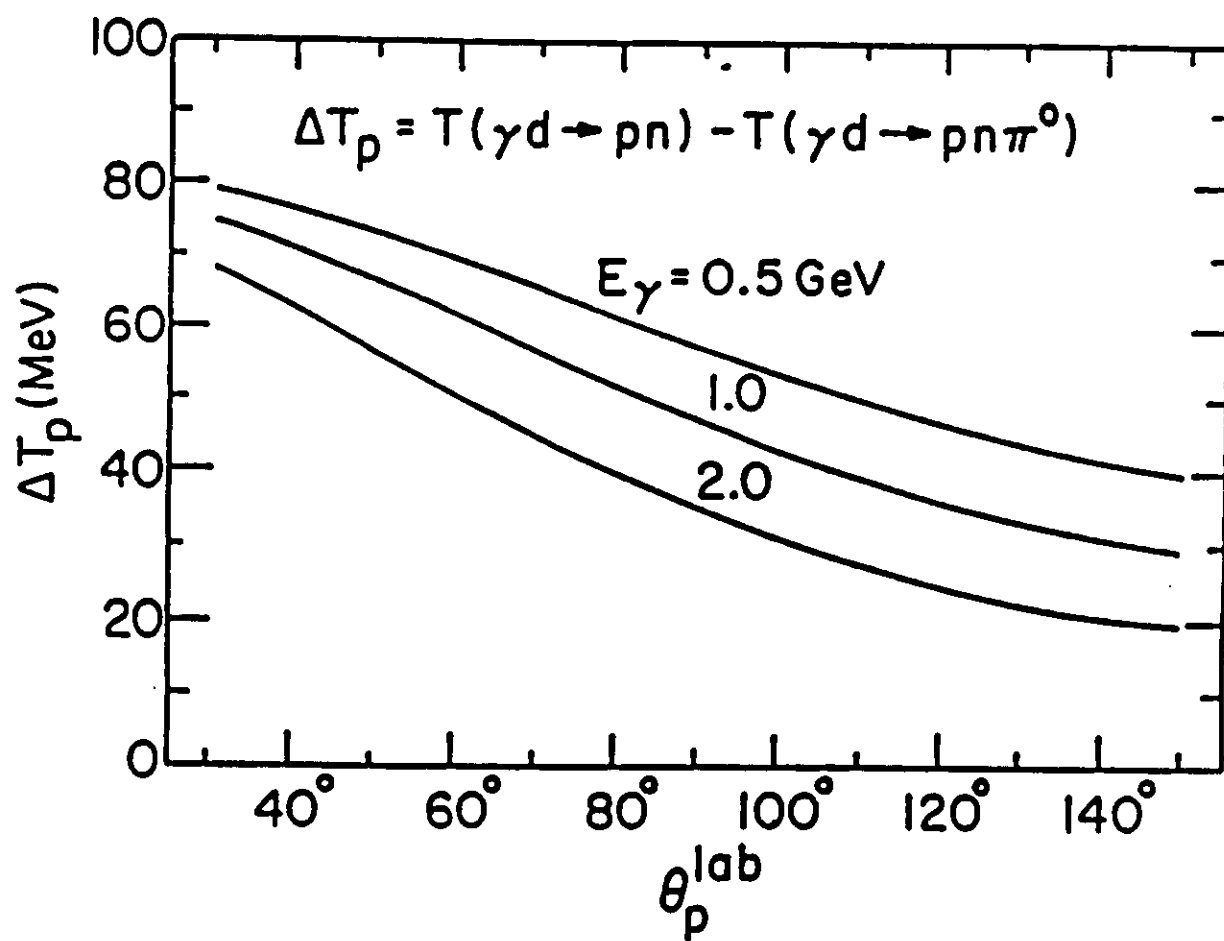
Figure 8. Difference in proton energy between the pn and pnπ⁰ final states for different incident photon energies E_γ

A second concern is the large cross sections for the three-body processes which will produce a high rate of pions in the trigger counter. The rate can be estimated as follows:

Beam intensity $=10^7/\text{sec}$

Total cross section$= 300 \; \mu\text{b}$

Target density $= 4.8 \times 10^{23} \; \text{at/cm}^2$

Singles rate$=(10^7/\text{sec})(300 \times 10^{-30} \; \text{cm}^2)(9/4\pi \; \text{sr})(4.8 \times 10^{23} \; \text{at/cm}^2)$

$\quad =1030/\text{sec}$

Although these events can be separated from the two-body reaction by momentum and time-of-flight analysis, they will create a high trigger rate that the processing of events would be impeded. On-line analysis with data from the wire chambers and tagging system should reduce this rate to about 100/sec before data is written for later analysis. Then 1000 hours of running will produce 3.6×10^8 events for off-line analysis.

A missing mass plot, comparing the event rate for different channels in the reaction, is given in Fig. 9. The plot shows the detector response at forward angles for the energy bin extending from 1.4 to 1.5 GeV. The pn final state is clearly distinguished from the competing reactions.

Polarized photons

In addition to the measurement of differential cross section, we propose to measure Σ, the cross-section asymmetry for linearly polarized photons

$$\Sigma = \frac{(d\sigma/d\Omega)^{\perp} - (d\sigma/d\Omega)^{\parallel}}{(d\sigma/d\Omega)^{\perp} + (d\sigma/d\Omega)^{\parallel}}$$

where $(d\sigma/d\Omega)^{\perp \, (\parallel)}$ is the differential cross section for the reaction with the photon polarization directed perpendicular (parallel) to the reaction plane. This measurement will be performed by replacing the radiator normally used in tagging bremsstrahlung with a crystal to produced polarized photons by interference effects.

Radiation from the crystal is due to both coherent and incoherent processes. An incoherent background is produced by lattice vibrations in the crystal. The coherent part is an enhancement over the incoherent background and rapidly increases with the energy of the incident electron. For a given electron energy, the coherent contribution decreases towards the high energy end of the photon spectrum where the photon energy equals the energy of the incident electron. The enhancement displays a strong peaked structure due to the lattice crystal structure. The peaks are
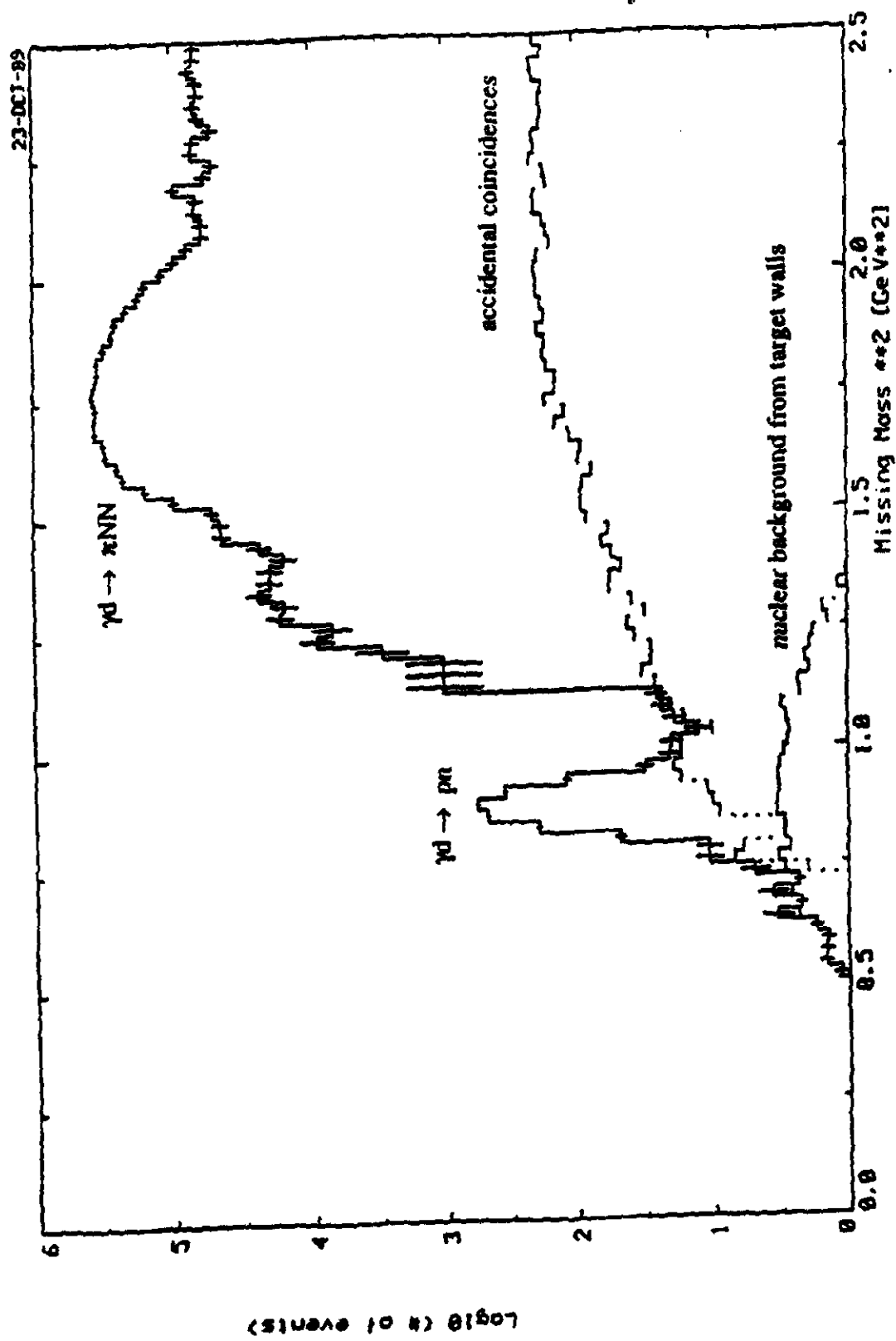
12

Figure 9. Missing mass plot of competing reactions for an electron beam energy of 1.6 GeV, a photon energy between 1.4 and 1.5 GeV and angles between 0° and 20°.

strongly polarized with a polarization which can be varied by changing the orientation of the crystal relative to the direction of the incident electron. A typical spectrum of the beam intensity and polarization for a 2 GeV electron beam on a diamond radiator is shown in Fig. 10.[40] Large polarizations are obtained at the low end of the bremsstrahlung spectrum.

By including the crystal in a tagging spectrometer, the angular position of the radiator can be verified by looking for peaks in the spectrum of tagged electrons. Because of its large angular acceptance, CLAS will be able to measure asymmetries for polarizations perpendicular and parallel to the reaction plane simultaneously.

Count rate estimate for polarized photons

The target and detector arrangement will be the same as for the measurement of differential cross section. Since the asymmetry parameter depends on a ratio of cross sections, a neutron coincidence requirement can be introduced into the trigger. Although the efficiency of the neutron counters is not well known, the efficiency will not affect the ratio of cross sections.

Inclusion of a neutron counter requirement will greatly reduce accidental background and allow operating at a higher rate. Since the neutron counters do not cover all angles uniformly, the event rate will depend on the angle of the neutron produced in the reaction. The rates relative to the rates given in Table I for the differential cross section with no neutron counter are shown in Table II. The relative rates include an increase in the beam intensity of a factor of 10.

Table II. Rates for polarization measurement relative to Table I.

Neutron Angle	Relative count rate
0°-45°	10x0.50 = 5
45°-90°	10x[0.5/6 + 0.05x(5/6)] = 1.25
90°-180°	10x0.05 = 0.5

We request 1000 hours to allow 3 angular settings of the crystal radiator for polarization measurements between 0.5 and 1 GeV.

Manpower

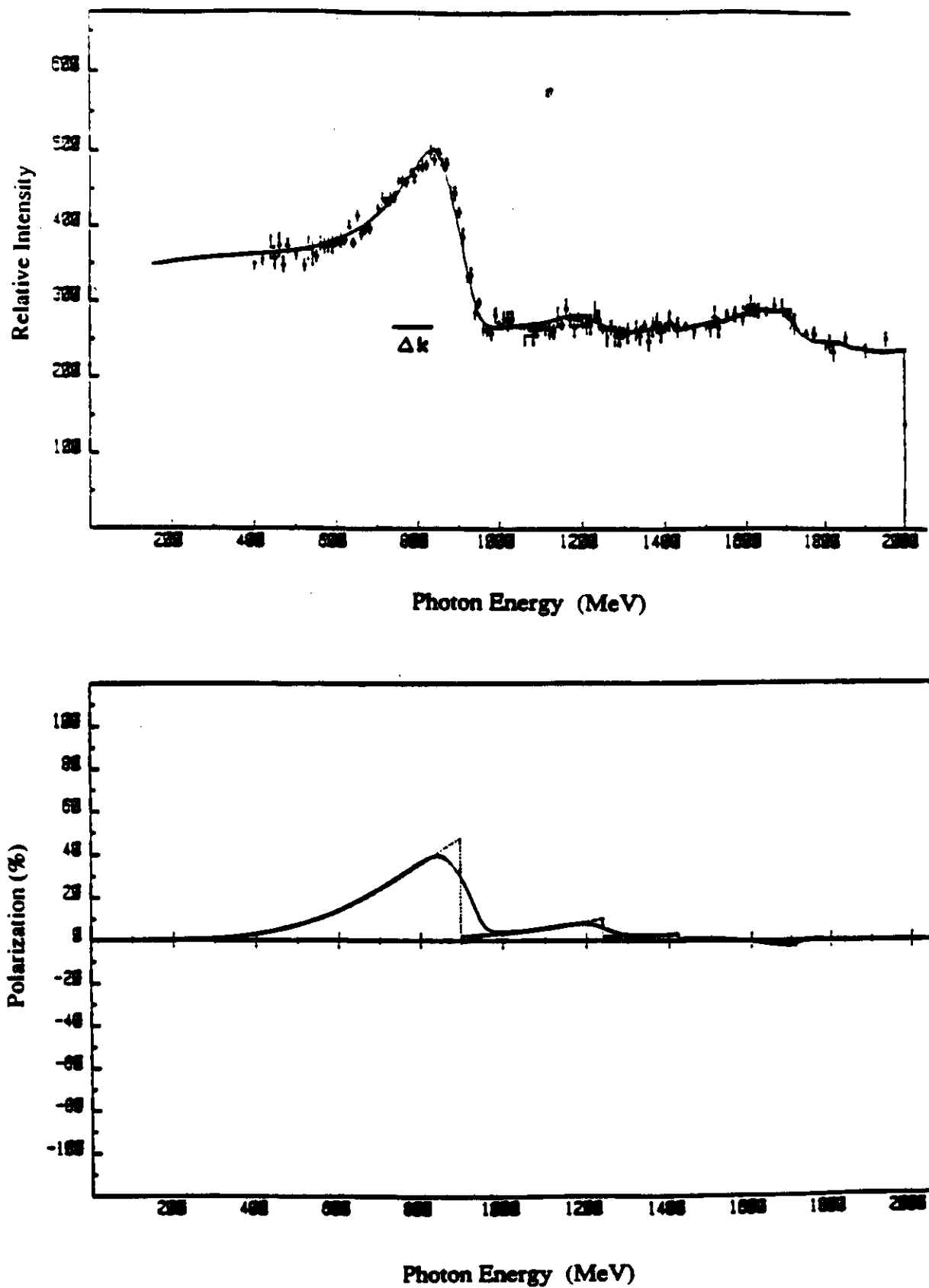The Photon Tagger Group will assist in the development of the photon beam, the whole collabo-

Figure 10. The intensity (top) and polarization (bottom) of photons produced by a 2 GeV electron beam incident upon a diamond radiator.

ration will participate in the data collection and the Virginia Tech and University of Virginia members will analyze the data.

Summary

We request 1000 hours for a measurement of the differential cross section over the energy range from 0.5 to 1.5 GeV. In this time we expect that data at the lower end of the energy range will have 2% statistics (neglecting background) accumulated in an angular bin of 5°and an energy bin of 5 MeV. The higher end of the energy range will have a statistical error of 2% for a 20°, 100 MeV energy bin.

In addition we request 1000 hours of data for measuring the asymmetry in the cross section between 0.5 and 1.0 GeV.

[1] J. Arends, H. J. Gassen, A. Hegerath, B. Mecking, G. Noldeke, P. Prenzel, T. Reichelt, A. Voswinkel, and W. W. Sapp, Nucl. Phys. A412, 509 (1984).

[2] K. Baba, I. Endo, H. Fukuma, K. Inoue, T. Kamamoto, T. Ohsugi, Y. Sumi, T. Takeshita, S. Uehara, Y. Yano, and T. Maki, Phys. Rev. Lett. 48, 729 (1982); Phys. Rev. C 28, 286 (1983).

[3] L. Craft. Ph.D. Thesis. Massachusetts Institute of Technology, Cambridge, MA. 1982.

[4] De Sanctis, Can. J. Phys. 62, 1083 (1984).

[5] F. Liu, D. E. Lundquist, and B. H. Wilk, Phys Rev. 65, 1478 (1968).

[6] K. Kose, B. Martin, R. Runkel, and H. Wahlen, Z. Phys. 220, 305 (1969).

[7] T. Kamae, I. Arai, T. Fujii, H. Ikeda, N. Kajiura, S. Kawabata, K. Nakamura, K. Ogawa, H. Takeda, and Y. Watase, Phys. Rev. Lett. 38, 468 (1977). K. Ikeda, L Arai, H. Fujii, T. Fujii, H. Iwasaki, N. Kajiura, T. Kamae, N. Nakamura, T. Sumiyoshi, H. Takeda, K. Ogawa, and M. Kanazawa, Nucl. Phys. B172, 509 (1980).

[8] Ishii, S. Kato, H. Okuno, K. Ukai, Y. Ohashi, N. Awahi, H. Hayashii, N. Horikawa, K. Kimusu, A. Miyamoto, T. Nakanishi, S. Okumi, H.Ozaki, A. Sugiyawa, R. Suzaki,T. Tauchi, K. Mori and Y.Takeuchi, Phys. Lett. 110B, 441 (1982).

[9] R. Ching and C. Schaerf, Phys. Rev. 1320, 141 (1966).

[10] H. Myers, R. Gomez, D. Guinier, and A. V. Tollestrup, Phys. Rev. 121, 630 (1961).

[11] P. Dougan, T. Kivikas, K. Lugner, V. Ramsay and W. Stiefler, Z. Physik A276, 55 (1976).

[12] K. H. Althoff, G. Anton, B. Bock, D. Bour, P.Erbs, W. Ferber, H. Gelhausen, U. Hartel, W. Havenith, T. Jahnen, H. P. Kaufmann, O. Kaul, B. Lucking, D. Menze, W. Meyer, T. Miczaika, K. Rennings, H. Riechert, E. Roderburg, W. Ruhmn, E. Scheniut, E. Schilling, W. Schwille, G. Sternal, D. Sundermann, W. Thiel, D. Thiesmeyer, and K. Wagener, Z. Phys. C 26, 175 (1984). See also BONN-ME-89-01, 1989.

[13] R. Brockmann et al. High-Energy Phys. Nucl. Struct. Proc. Int. Conf., 8th Vancouver, B. C. 1979; V. G. Gorbenko, Yu V. Zhebrovskii, L. Ya Kolesnikov, A. L. Rubashkin, and P. V. Sorokin. Pis'ma Zh. Eksp. Teor. Fiz. 30, 130 (1979); JETP Lett. (Engl. Transl.), 30, 118 (1979).

[14] V. G. Gorbenko, Yu. V. Zhebrovskii, L. Ya. Kolesnikov, A. L. Rubashkin, and P. V. Sorkin, Nucl. Phys. A381, 330 (1982).

[15] V. P. Barannik, A. S. Bratashevskij, V. G. Gorbenko, V. A. Gushchin, Yu.V. Zhebrovskij, A. A. Zybalov, S. P. Karasev, L. Ya. Kolesnikov, O. G. Konovalov, Yu.V. Kulish, M. P. Rekalo, A. L. Rubashkin, P. V. Sorokin, Yu.O. Storozhenko and A.Eh. Tenishev "Proton Polarization in Deuteron Disintegration by Linearly Polarized Photons and Dibaryon Resonances", Nucl. PHys. A451, 751 (1986).

[16] K. Sh. Agababyan, F. V. Adamyan, G. G. Akopyan, G. A. Vartapetyan, P. I. Galumyan, V. O. Grabskii, V. V. Karapetyan, G. V. Karapetyan and M. S. Kordonskii, Yad. Fiz. 41, 1401 (1985); Sov. J. Nucl. Phys. (Engl. Transl.), 41, 888 (1985).

[17] A. Bratashevskii, A. I. Derebchinskii, A. A. Zybalob, O. T. Konovalov, P. V. Sorokin, and A. E. Tenishev, Yad. Fiz 32, 418 (1980); Sov. J. Nucl. Phys. (Engl Transl.), 32, 216 (1980).

[18] R. J. Holt et al., "Two-Body Photodisintegration of the Deuteron Above 1 GeV", Argonne Report PHY-5266-ME-88, 1988.

[19] W. Schwille, reported at the CEBAF 1986 Summer Workshop.

[20] H. O. Meyer, J. R. Hall, M. Hugi, H. J. Karwowsky, R. E. Pollock and P. Schwandt, Phys. Rev. C31, 309 (1985).

[21] J. M. Cameron, C. A. Davis, H. Fielding, P. Kitching, J. Pasos, J. Soukup, J. Uegaki, J.

Weisick, H. S. Wilson, R. Abegg, D. A. Hutcheon, C. A. Miller, A. W. Stetz and I. J. Van Heerden, Nucl. Phys. A458, 637 (1986). See also Nucl. Phys. A472, 701 (1987).

[22]   E. DeSanctis "A Critical Review of Deuteron Photodisintegration Data", LNF-88/54(P), 1988.

[23]   J. M. Cameron, Can. J. Phys. 62, 1019 (1984).

[24]   W. Pfeil, report to the 1986 Summer Workshop.

[25]   W. Leidemann and H. Arenhovel, "Two-Body Deuteron Photodisintegration Above Pion Threshold With A Dynamical Treatment of Δ Degrees of Freedom", submitted for publication.

[26]   K. Ogawa, T. Kamae and K. Nakamura "Theoretical Models for Deuteron Photodisinte-gration in the Energy Range Between 250 MeV and 800 MeV", Nucl. Physics A340, 451 (1980)

[27]   O. I. Dahl, N. Horwitz, D. H. Miller, J. J. Murphy and P. G. White, Phys. Rev. 6, 142 (1961).

[28]   R. A. Arndt, Phys. Rev. 165, 1834 (1968).

[29]   R. L. Shypit et al., Phys. Rev. Lett 60, 901 (1988).

[30]   K. Hidaka, *Comment on "Evidence Against Broad Dibaryons"*, Report TGU-6, Tokyo Gakugei University, July 1989.

[31]   S. J. Brodsky and J. R. Hiller, Phys. Rev. C 28, 475 (1983).

[32]   S. J. Brodsky and B. T. Chertok, PR D14, 3003 (1976).

[33]   N. Isgur and C. H. L. Smith, Phys Rev Let 52, 1080 (1984).

[34]   C. Carlson and F. Gross, Phys Rev Let. 53, 127 (1984).

[35]   Techniques for producing a tagged photon beam are reviewed by L. S. Cardman, *Photon Tagging, Present Practice and Future Prospects*, Proceedings of the Magnetic Spectrometer Workshop, Williamsburg, Virginia, 1983.

[36]   R. M. Laszewski, July 1980 Report of the Nuclear Physics Laboratory, University of Illinois, 42, (1980).

[37]   W. Meyer, *Polarized Proton and Deuteron Targets*, Proceedings of the 1985 CEBAF Summer Workshop, Newport News, Virginia, page 237.

[38]   M. W. McNaughton, *Proton Polarimeters for Spin Transfer Experiments*, Proceedings of the CEBAF 1985 Summer Workshop, Newport News, Virginia, page 271.

[39]   R. Madey, J. W. Watson, B. D. Anderson, A. R. Baldwin and P. J. Pella "Neutron Pola-rimeters", Report of the June 1985 CEBAF Summer Workshop.

[40]   Ernst A. Dahl, *Experimental Determination of the Asymmetry Σ of the differential cross section for deuteron photodisintegration γ + d → p + n with linearly polarized photons in the energy range 230 - 820 MeV*, Bonn-IR-82-26, 1982.